Article

Investigation of Photocatalysis by Mesoporous Titanium Dioxide Supported on Glass Fibers as an Integrated Technology for Water Remediation

Cristina De Ceglie [1,†], Sudipto Pal [2,*,†], Sapia Murgolo [1], Antonio Licciulli [2] and Giuseppe Mascolo [1,*]

[1] Istituto di Ricerca sulle Acque, National Council Research, Via F. De Blasio 5, 70132 Bari, Italy; cristina.deceglie@ba.irsa.cnr.it (C.D.C.); sapia.murgolo@ba.irsa.cnr.it (S.M.)
[2] Department of Innovation Engineering, University of Salento, Via Per Monteroni, Lecce, Italy;
antonio.licciulli@unisalento.it
* Correspondence: sudipto.pal@unisalento.it (S.P.); giuseppe.mascolo@ba.irsa.cnr.it (G.M.)
†

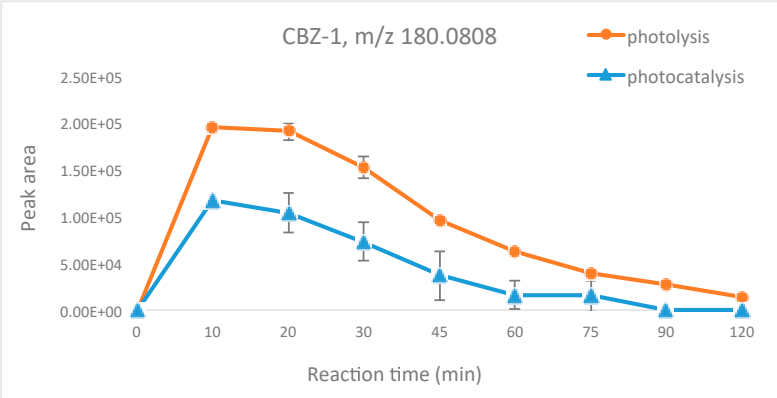

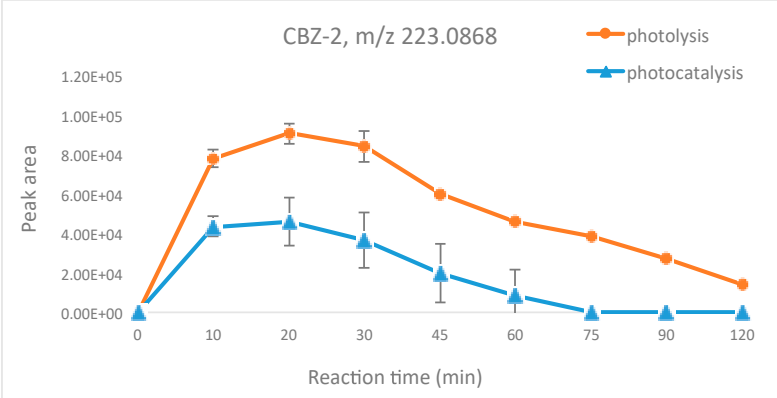

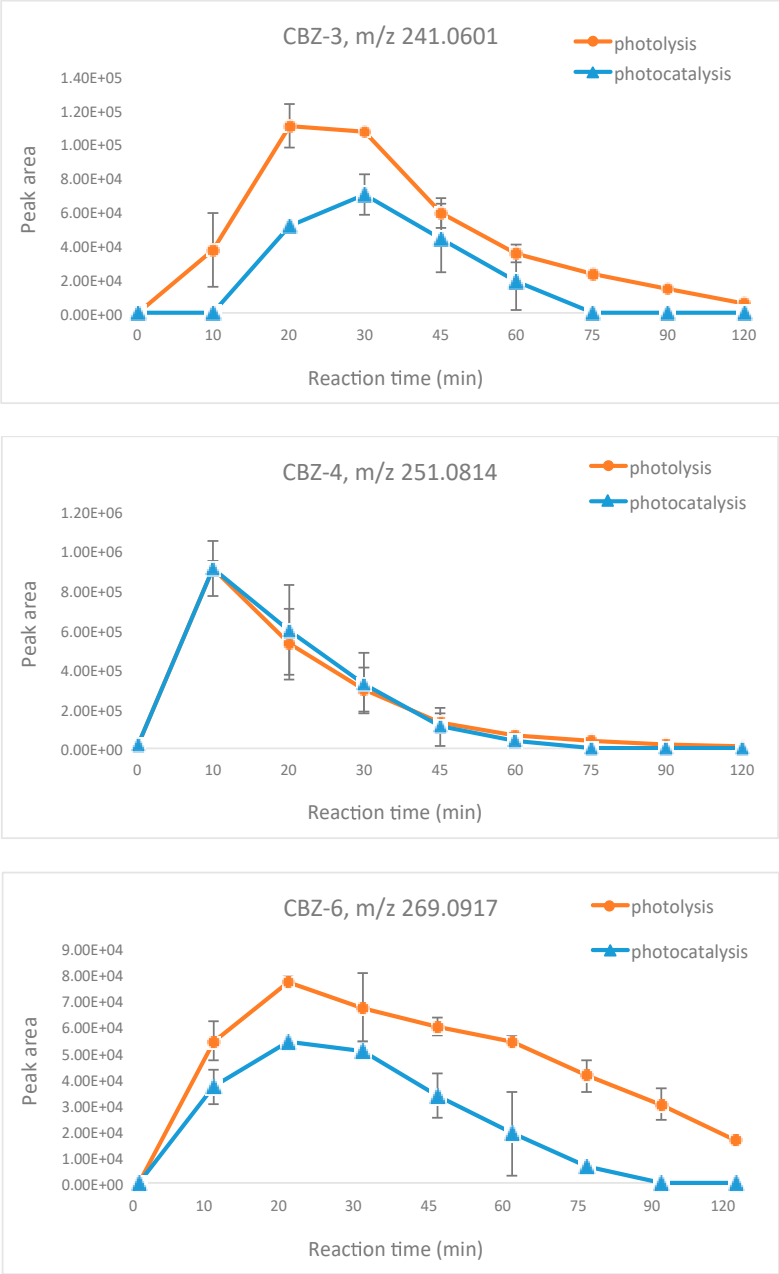

Figure S1. Time profiles of CBZ TPs during photolysis and photocatalysis with mesoporous TiO_2 coated on glass fibers, using secondary wastewater effluent.

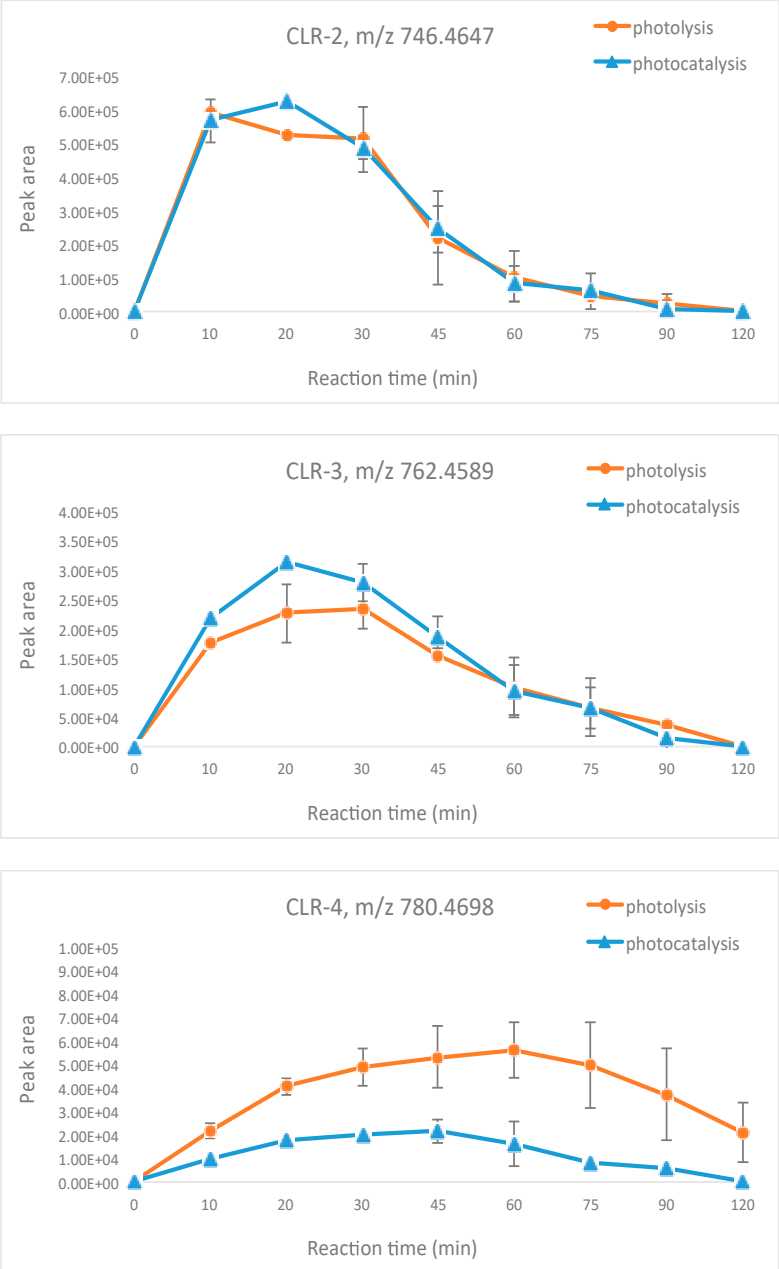

Figure S2. Time profiles of CLR TPs during photolysis and photocatalysis with mesoporous TiO_2 coated on glass fibers, using secondary wastewater effluent.

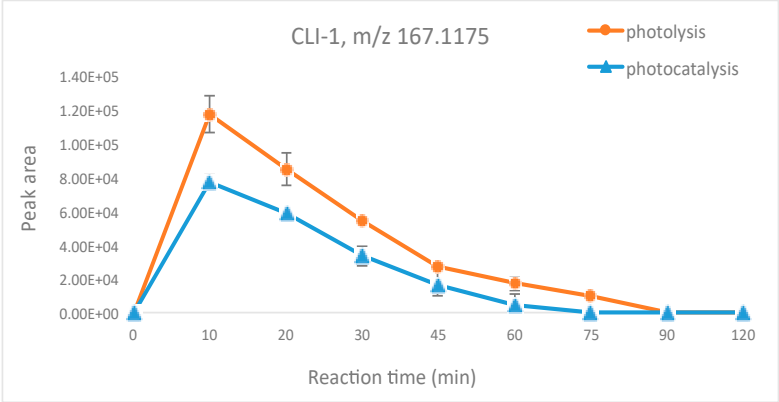

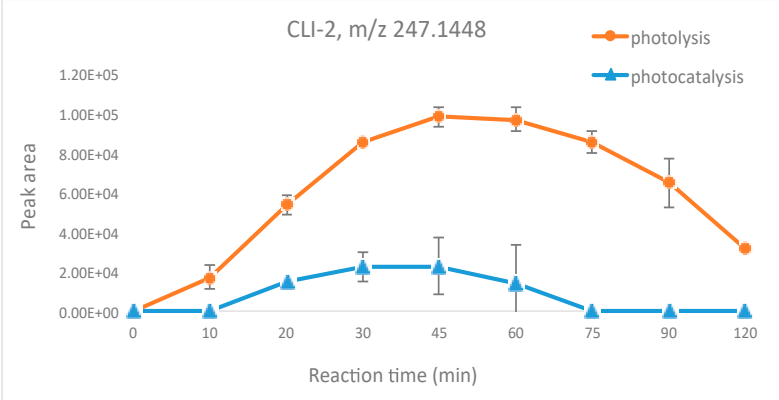

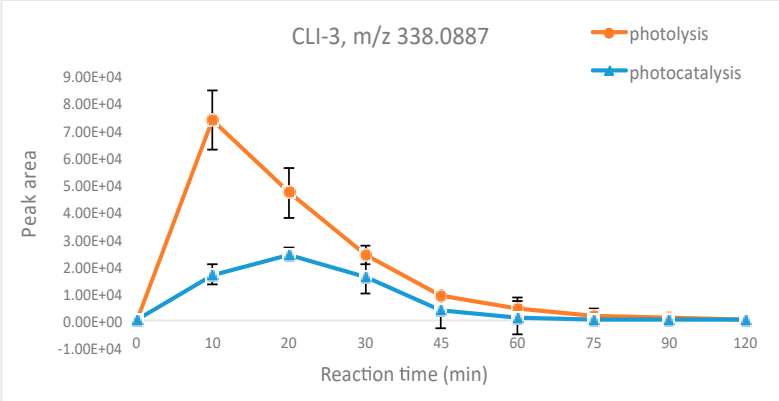

Figure S3. Time profiles of CLI TPs during photolysis and photocatalysis with mesoporous TiO_2 coated on glass fibers, using secondary wastewater effluent.

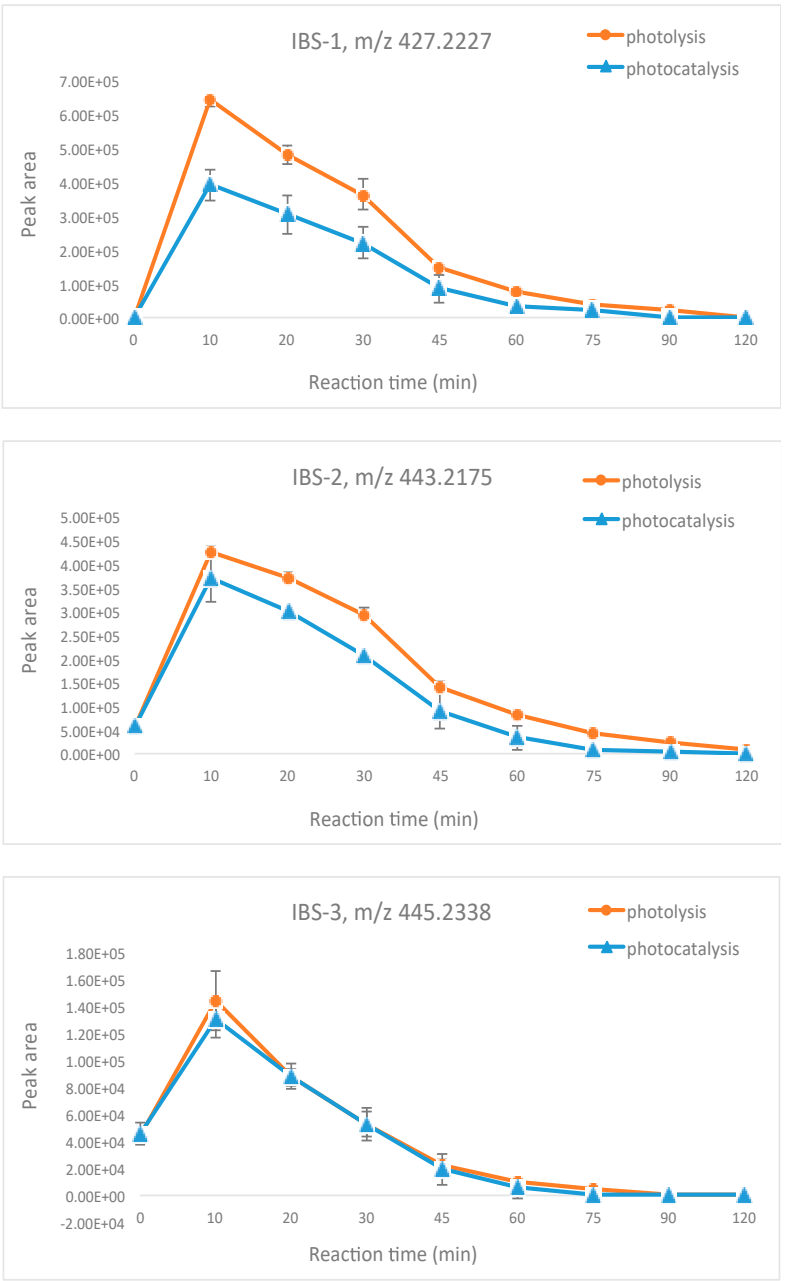

Figure S4. Time profiles of IBS TPs during photolysis and photocatalysis with mesoporous TiO_2 coated on glass fibers, using secondary wastewater effluent.

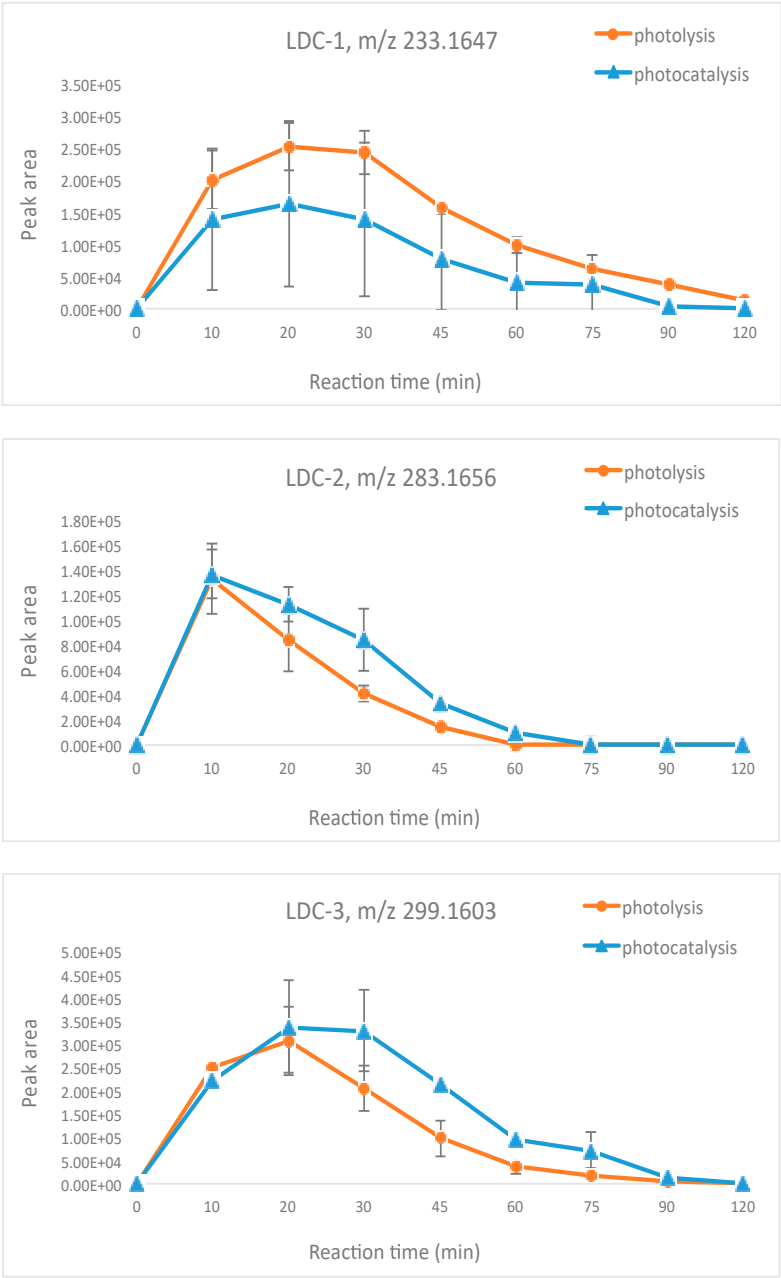

Figure S5. Time profiles of LDC TPs during photolysis and photocatalysis with mesoporous TiO_2 coated on glass fibers, using secondary wastewater effluent.

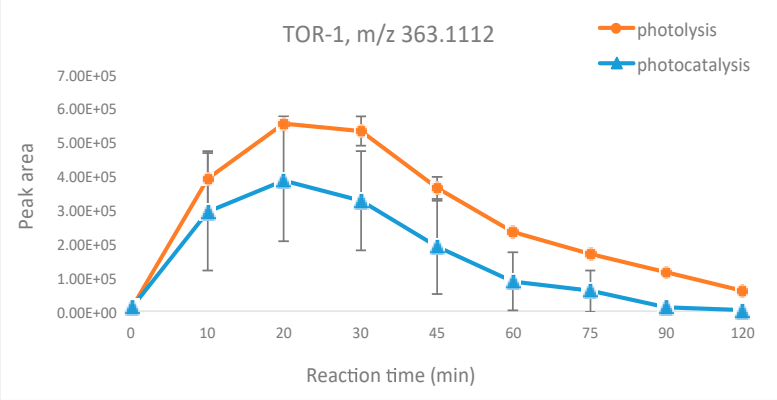

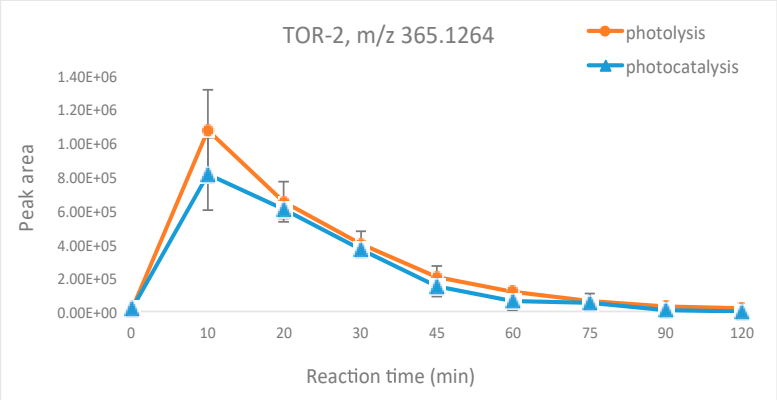

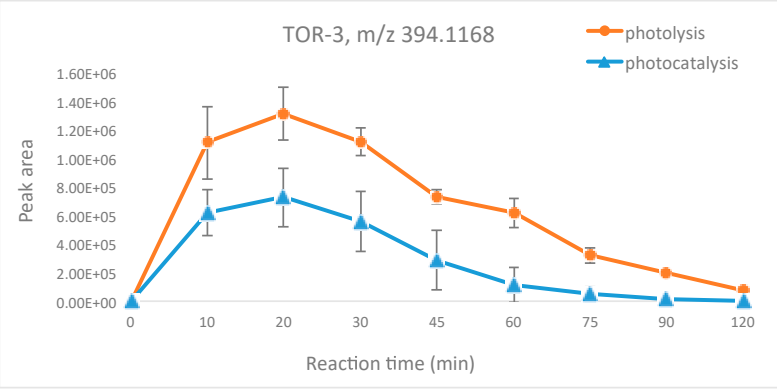

Figure S6. Time profiles of TOR TPs during photolysis and photocatalysis with mesoporous TiO_2 coated on glass fibers, using secondary wastewater effluent.

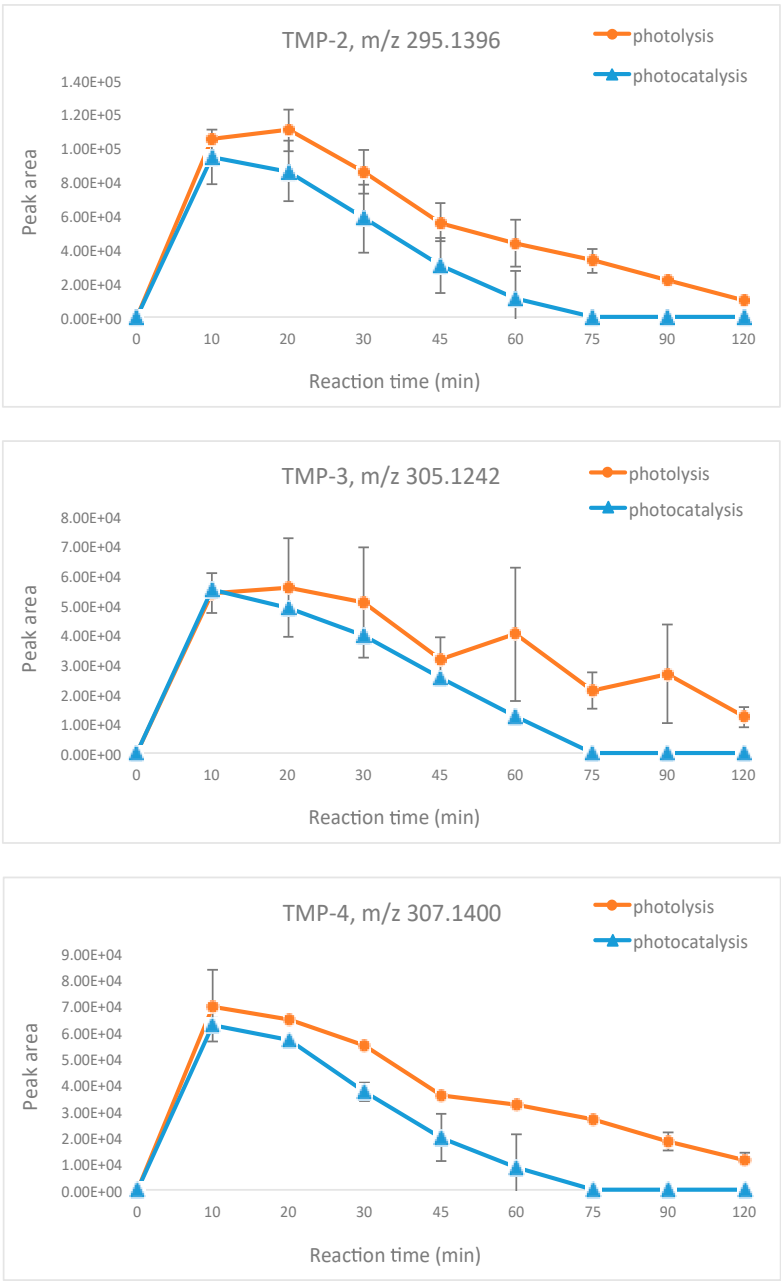

Figure S7. Time profiles of TMP TPs during photolysis and photocatalysis with mesoporous TiO_2 coated on glass fibers, using secondary wastewater effluent.

Table S1. List of transformation products of the *spiked compounds* detected by suspect screening in photolytic and photocatalytic experiments (mesoporous TiO_2 supported on glass fibers), treating secondary wastewater effluent.

	Metabolite	Measured *m/z*, $[M+H]^+$	RT (min)	Empirical Formula	Modification (mass shift)	References	Proposed structure
Carbamazepine **(m/z 237.1014)**	TP1 (CBZ-1) Acridine	180.0808	5.11	$C_{13}H_9N$	Loss of CHNO+Demethylation (-57.02)	[41]	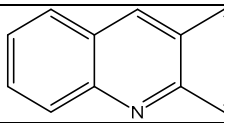
Carbamazepine	TP2 (CBZ-2)	223.0868	8.14	$C_{14}H_{10}N_2O$	Demethylation (-14.01)	[39,40]	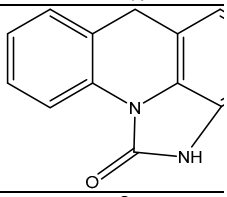
Carbamazepine	TP3 (CBZ-3)	241.0601	6.91	$C_{13}H_8N_2O_3$	Deethylation and Carboxylic Acid Formation (3.95)	New TP	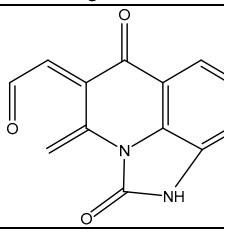
Carbamazepine	TP4 (CBZ-4)	251.0814	7.16	$C_{15}H_{10}N_2O_2$	Ketone Formation (13.98)	[39,40]	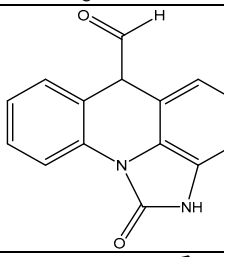
Carbamazepine	TP5 (CBZ-5)	267.0765	7.89	$C_{15}H_{10}N_2O_3$	Demethylation to Carboxylic Acid (29.97)	[39–41]	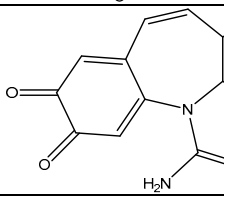
Carbamazepine	TP6 (CBZ-6)	269.0917 (H isomer)	7.40	$C_{15}H_{12}N_2O_3$	Di-Oxidation (31.99)	[39–41]	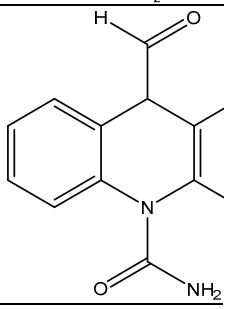

	Metabolite	Measured *m/z*, $[M+H]^+$	RT (min)	Empirical Formula	Modification (mass shift)	References	Proposed structure
Clarithromycin **(m/z 748.4762)**	TP7 (CLR-1)	622.3769	5.70	$C_{30}H_{55}NO_{12}$	Loss of $C_8H_{14}O_3$+Di-Oxidation (-126.09)	[39]	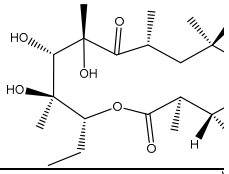
Clarithromycin	TP8 (CLR-2)	746.4647	7.78	$C_{38}H_{67}NO_{13}$	Desaturation (-2.01)	[39]	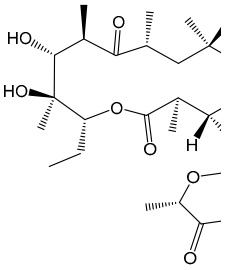
Clarithromycin	TP9 (CLR-3)	762.4589	7.53	$C_{38}H_{67}NO_{14}$	Ketone Formation (13.98)	[39,42]	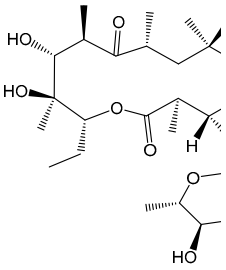
Clarithromycin	TP10 (CLR-4)	780.4701	6.71	$C_{38}H_{69}NO_{15}$	Di-Oxidation (31.99)	[39]	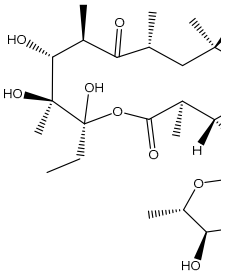
Climbazole **(m/z 293.1050)**	TP11 (CLI-1)	167.1175	4.51	$C_9H_{14}N_2O$	Loss of C_6H_3OCl (-125.98)	[43]	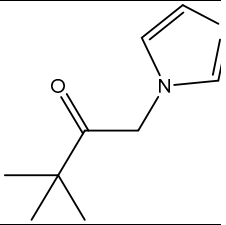
Climbazole	TP12 (CLI-2)	247.1448	8.11	$C_{14}H_{18}N_2O_2$	Loss of Cl->H+Demethylation and Hydrogenation (-45.96)	New TP	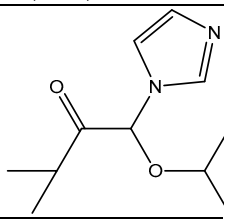

	Metabolite	Measured *m/z*, $[M+H]^+$	RT (min)	Empirical Formula	Modification (mass shift)	References	Proposed structure
Climbazole	TP13 (CLI-3)	338.0887	6.71	$C_{15}H_{16}N_3O_4Cl$	Nitro climbazole (44.98)	New TP	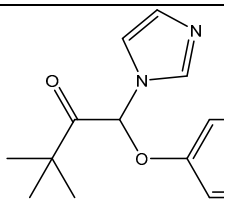
Irbesartan **(m/z 429.2362)**	TP14 (IBS-1)	427.2227	10.37	$C_{25}H_{26}N_6O$	Desaturation (-2.01)	[47]	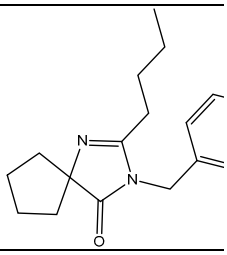
Irbesartan	TP15 (IBS-2)	443.2175	8.07	$C_{25}H_{26}N_6O_2$	Ketone Formation (13.98)	[46]	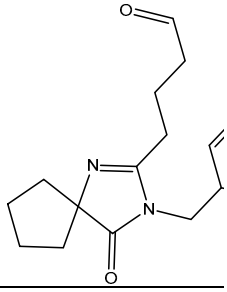
Irbesartan	TP16 (IBS-3)	445.2338	7.23	$C_{25}H_{28}N_6O_2$	Oxidation (15.99)	New TP	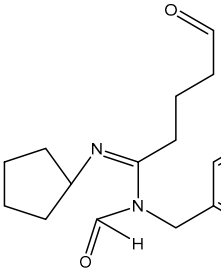
Lidocaine **(m/z 235.1794)**	TP17 (LDC-1)	233.1647	5.88	$C_{14}H_{20}N_2O$	Desaturation (-2.01)	New TP	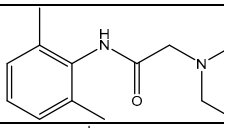
Lidocaine	TP18 (LDC-2)	283.1656	3.25	$C_{14}H_{22}N_2O_4$	Tri-Oxidation (47.98)	New TP	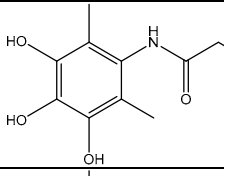
Lidocaine	TP19 (LDC-3)	299.1603	3.02	$C_{14}H_{22}N_2O_5$	Tetra-Oxidation (63.98)	New TP	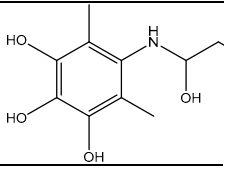

	Metabolite	Measured *m/z*, $[M+H]^+$	RT (min)	Empirical Formula	Modification (mass shift)	References	Proposed structure
Torsemide **(m/z 349.1306)**	TP20 (TOR-1)	363.1112	7.73	$C_{16}H_{18}N_4O_4S$	Ketone Formation (13.98)	[49]	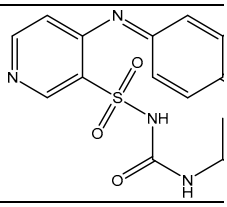
Torsemide	TP21 (TOR-2)	365.1264	5.83	$C_{16}H_{20}N_4O_4S$	Oxidation (15.99)	[49]	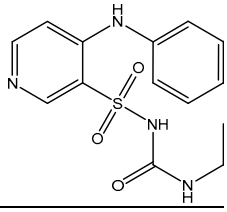
Torsemide	TP22 (TOR-3)	394.1168	7.27	$C_{16}H_{19}N_5O_5S$	Nitro torsemide (44.98)	[49]	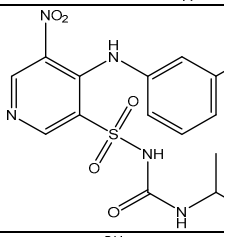
Trimethoprim **(m/z 291.1439)**	TP23 (TMP-1) 3-desmethyl-TMP	277.1291	6.27	$C_{13}H_{16}N_4O_3$	Demethylation (-14.01)	[38]	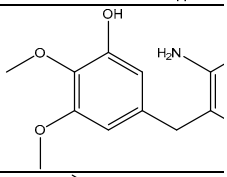
Trimethoprim	TP24 (TMP-2)	295.1396	4.64	$C_{13}H_{18}N_4O_4$	Loss of CH2+Internal Hydrolysis (3.99)	[38]	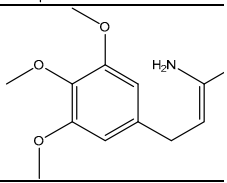
Trimethoprim	TP25 (TMP-3)	305.1242	5.08	$C_{14}H_{16}N_4O_4$	Ketone formation (13.98)	[38]	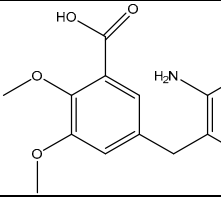
Trimethoprim	TP26 (TMP-4)	307.1400	4.68	$C_{14}H_{18}N_4O_4$	Oxidation (15.99)	[38]